Bimodal anti-glioma mechanisms of cilengitide demonstrated by novel invasive glioma models

Running title: Bimodal anti-glioma mechanisms of cilengitide

Manabu Onishi, MD[1], Tomotsugu Ichikawa, MD, PhD[1], Kazuhiko Kurozumi, MD, PhD[1], Kentaro Fujii, MD[1], Koichi Yoshida, MD[1], Satoshi Inoue, MD, PhD[1], Hiroyuki Michiue, MD, PhD[1], E. Antonio Chiocca, MD, PhD[2], Balveen Kaur, PhD[2], Isao Date, MD, PhD[1]

[1]Department of Neurological Surgery, Okayama University Graduate School of Medicine, Dentistry and Pharmaceutical Sciences, 2-5-1, Shikata-cho, Kita-ku, Okayama, 700-8558, Japan.

[2]Dardinger Laboratory for Neuro-oncology and Neurosciences, Department of Neurological Surgery, The Ohio State University, N-1017 Doan Hall, Columbus, OH 43210, USA.

Corresponding author contact information

Tomotsugu Ichikawa, M.D., Ph.D.

Department of Neurological Surgery, Okayama University Graduate School of Medicine, Dentistry and Pharmaceutical Sciences

Address: 2-5-1 Shikata-cho, Kita-ku, Okayama, 700-8558, Japan

Phone: +81-86-235-7336

Fax: +81-86-227-0191

E-mail: tomoichi@cc.okayama-u.ac.jp

Abstract

Background: Integrins are expressed in tumor cells and tumor endothelial cells, and likely play important roles in glioma angiogenesis and invasion.

Objective: We investigated the anti-glioma mechanisms of cilengitide (EMD121974), an αvβ3 integrin inhibitor, utilizing the novel invasive glioma models, J3T-1and J3T-2.

Methods and results: Immunohistochemical staining of cells in culture and brain tumors in rats revealed positive αvβ3 integrin expression in J3T-2 cells and tumor endothelial cells, but not in J3T-1 cells. Established J3T-1 and J3T-2 orthotopic gliomas in athymic rats were treated with cilengitide or solvent. J3T-1 gliomas showed perivascular tumor cluster formation and angiogenesis, while J3T-2 gliomas showed diffuse single-cell infiltration without obvious angiogenesis. Cilengitide treatment resulted in a significantly decreased diameter of the J3T-1 tumor vessel clusters and its core vessels when compared with controls, while an anti-invasive effect was shown in the J3T-2 glioma with a significant reduction of diffuse cell infiltration around the tumor center. The survival of cilengitide-treated mice harboring J3T-1 tumors was significantly longer than that of control animals (median survival; 57.5 days and 31.8 days, respectively, $P < 0.005$), while cilengitide had no effect on the survival of mice with J3T-2 tumors (median survival; 48.9 days and 48.5, $P = 0.69$).

Conclusion: Our results indicate that cilengitide exerts a phenotypic anti-tumor effect by inhibiting angiogenesis and glioma cell invasion. These two mechanisms are clearly shown by the experimental treatment of two different animal invasive glioma models.

Key words

angiogenesis; animal model; glioma; integrin; invasion

Introduction

Gliomas are the most frequent primary intracranial neoplasm in adults, and are invariably fatal. The median survival of aggressively treated patients with glioblastoma multiforme (GBM) is approximately 14.6 months[1]. The resistance of gliomas to the conventional therapeutic regimen of surgery, radiotherapy, and chemotherapy has prompted many investigators to seek novel therapeutic approaches for this fatal disease[2].

Two major aspects of glioma biology are the formation of new blood vessels through angiogenesis and the invasion of glioma cells via white matter tracts, which are the hallmarks of GBM[3]. The formation of abnormal tumor vasculature is one of the major reasons for the resistance of these tumors to treatment[4]. Inhibitors of angiogenesis can suppress tumor growth in preclinical models and have entered the clinic as prospective anticancer therapeutics[5]. Specifically, the administration of bevacizumab, a humanized monoclonal antibody against vascular endothelial growth factor (VEGF), in combination with irinotecan, a topoisomerase inhibitor, significantly improves outcome among recurrent patients[6,7]. However, de Groot et al.[8] showed that glioma cases developed an apparent phenotypic shift to a predominantly infiltrative pattern of tumor progression after treatment with bevacizumab. Thus, in addition to anti-angiogenesis therapy, successful treatment strategies for GBM may require the concomitant targeting of tumor cell invasion[9].

Integrins are expressed in tumor cells and tumor endothelial cells[10], and they play important roles in angiogenesis and invasion in gliomas[11-13]. αvβ3 and αvβ5 integrins regulate cell adhesion[14,15], and inhibitors of these integrins suppress tumor growth in certain pre-clinical models[16]. Therefore, integrins are being investigated as therapeutic targets in gliomas.

Cilengitide (EMD121974), a cyclic arginine-glycine-aspartic acid pentapeptide, is an αvβ3 integrin antagonist that induces anoikis in angiogenic blood vessels and brain tumor

cells *in vitro*[17,18]. Cilengitide may inhibit tumor growth by at least two mechanisms: by targeting the tumor cells directly and by inhibiting tumor angiogenesis[2,17,19]. However, these mechanisms were not elucidated in invasive brain tumor models in animals.

We have established two new cell line-based animal models of invasive glioma, J3T-1 and J3T-2. These animal models histologically recapitulate two invasive and angiogenic phenotypes, namely angiogenesis-dependent and -independent invasion, which is also observed in human glioblastoma[4,20]. In short, J3T-1 cells form well demarcated and highly angiogenic tumors in rat brains, and clusters of tumor cells are seen around dilated, newly developed vessels in the adjacent normal brain. Therefore, J3T-1 gliomas express angiogenesis-dependent invasion and growth. In contrast, J3T-2 cells form poorly demarcated tumors, where the tumor cells gradually disperse from the tumor center to the normal brain parenchyma. Single cells also invade the normal brain parenchyma along white matter tracts. Therefore, J3T-2 gliomas express angiogenesis-independent invasion and growth.

To our knowledge, there are no published data demonstrating the anti-angiogenic or anti-invasive effects of cilengitide on gliomas using invasive animal models. Investigating the effects of cilengitide poses a challenge because most of the conventional animal models fail to mimic the invasiveness and angiogenesis of human glioma. Here, we investigated the antitumor effects of cilengitide on two experimental animal models of malignant glioma, J3T-1 and J3T-2.

Materials and Methods

Glioma cell lines

Two cell lines, J3T-1 and J3T-2, were developed from the same parental J3T canine glioma cell line (a generous gift from Dr. Michael E. Berens; Translation Genomics Research Institute, Phoenix, AZ, USA), as previously described[4,21]. J3T-1 cells and J3T-2 cells were

seeded on tissue culture dishes (BD Falcon, Franklin Lakes, NJ, USA) and cultured in Dulbecco's Modified Eagle's Medium (DMEM) supplemented with 10% fetal bovine serum (FBS), 100 units of penicillin and 0.1 mg of streptomycin per milliliter.

Cell surface immunofluorescence assay

J3T-1 and J3T-2 cells were seeded onto four chamber polystyrene vessel tissue culture treated glass slides (BD Falcon) and incubated overnight. For immunofluorescence, the cells were fixed in 4% paraformaldehyde in phosphate-buffered saline (PBS) for 15 min. After the cells were fixed, they were rinsed three times with PBS. Nonspecific binding was blocked by incubation in a blocking buffer containing 2% bovine serum albumin (BSA) in PBS for 30 min at room temperature. The cells were incubated overnight at 4°C with a mouse monoclonal anti-αvβ3 integrin antibody (Millipore Corporation, Billerica, MA, USA) diluted 1:100 in blocking buffer. The cells were washed three times in blocking buffer for 5 min before incubation with a secondary anti-mouse CY3-conjugated antibody (Jackson ImmunoResearch Laboratories, Inc., West Grove, PA, USA) diluted 1:300 in blocking buffer for 2 h at room temperature in the dark. After three washes in PBS, the cells were counterstained with 4′, 6-diamino-2-phenylindole (DAPI; 1:500) (Invitrogen, Carlsbad, CA, USA) (100 ng/mL) for 20 min at room temperature. The slides were washed three times in PBS and mounted.

Tube formation assay

An angiogenesis assay kit (Kurabo, Osaka, Japan) was used according to the manufacturer's instructions. Briefly, human umbilical vein endothelial cells (HUVECs), co-cultured with neonatal normal human dermal fibroblasts (NHDFs)[22], were treated with various concentrations of cilengitide (0, 0.1, 0.5, or 1.0, or 2.0 μM) and VEGF (10 ng/mL)

added to the medium. Cilengitide was generously provided by Merck Serono and the National Cancer Institute, NIH. Suramin (50 μM) was used as a positive anti-angiogenic control. The medium was changed every three days. After ten days, the dishes were washed with PBS and fixed with 70% ethanol at 4°C. After the fixed cells were rinsed three times with PBS, the cells were incubated with mouse anti-human CD31 antibody (Kurabo, Osaka, Japan) diluted 1:4000 in PBS containing 1% BSA for 60 min. After washing three times with 1% BSA-PBS, the cells were incubated with goat anti-mouse IgG-alkaline phosphatase conjugate. Metal-enhanced 3, 3′-diamino-benzidine-tetrahydrochloride (DAB) was used as the substrate with the reaction yielding a dark reddish-brown insoluble end-product. Finally, the cells were washed five times with PBS and viewed under a microscope (BZ-8000, Keyence, Osaka, Japan). The area and tube length were measured quantitatively with the Kurabo angiogenesis image analyzer in five different fields per well and statistically analyzed[23].

Effects of cilengitide on cultured glioma cells

J3T-1 and J3T-2 cells were seeded on 6 well plates (1.0×10^4 cells/well) and cultured in DMEM supplemented with 10% FBS. Cilengitide (0, 0.1, 0.5, or 1.0 μM) was added to the medium after 24 h of incubation. Each experiment was performed in triplicate. After incubation for 120 h at 37°C, the cells were examined for morphological changes. Non-adherent cells were removed by gentle washing twice with PBS, and the attached cells were then trypsinized and counted. The cell counts at 24 and 120 h incubation were compared and the cell proliferation rate was calculated[17]. Apoptotic cells were detected with the In Situ Cell Death Detection Kit (Roche, Basel, Switzerland) according to the manufacturer's instructions.

Invasive glioma xenograft models

All experimental animals were housed and handled in accordance with the guidelines of the Okayama University Animal Research Committee. Before implantation, 85–90% confluent J3T-1 and J3T-2 cells were trypsinized, rinsed with DMEM supplemented with 10% FBS, and centrifuged at 100×g for 5 min. The resulting pellet was then resuspended in PBS, and the cell concentration was adjusted to 1.0×10^5 cells/μL. For each cell line, athymic rats (F344/N-nu/nu; CLEA Japan, Inc., Tokyo, Japan) were injected with 5 μL J3T-1 or J3T-2 cells and athymic mice (balb/c-nu/nu; CLEA Japan, Inc, Tokyo, Japan) were injected with 2 μL J3T-1 or J3T-2 cells. The animals were anesthetized and placed in stereotactic frames (Narishige, Tokyo, Japan) with their skulls exposed. Tumor cells were injected with a Hamilton syringe (Hamilton, Reno, NV, USA) into the right frontal lobe (in the athymic rats: 4 mm lateral and 1 mm posterior to the bregma at a depth of 4 mm; in the athymic mice: 3 mm lateral and 1 mm anterior to the bregma at a depth of 3 mm), and the syringe was slowly withdrawn after 5 min to prevent reflux. The skulls were then cleaned, the holes were sealed with bone wax, and the incision was sutured.

Cilengitide or PBS was administered three times/week intraperitoneally (for the athymic mouse: 200 μg/100 μL PBS; for the athymic rat: 1000 μg/500 μL PBS) starting on day five after tumor cell implantation. To analyze survival time, the J3T-1 and J3T-2 athymic mice xenograft models were monitored.

Histopathological analysis of glioma in rats

For histopathological analysis, athymic rats harboring J3T-1 or J3T-2 brain tumors were sacrificed at 35 days after tumor implantation. Before being sacrificed for immunohistochemistry and hematoxylin and eosin (HE) staining, athymic rats were anesthetized, euthanized by cardiac puncture, perfused with 100 mL PBS, and fixed with 200

mL 4% paraformaldehyde. The brains were removed and stored in 4% paraformaldehyde for at least 24 h.

For HE staining, the sections were immersed in hematoxylin for 1 min and rinsed with tap water. The sections were then immersed in an eosin stain for 1–2 min and rinsed with tap water.

For immunohistochemical staining of αvβ3 integrin, after deparaffinization in xylene and rehydration in decreasing concentrations of ethanol, 4-μm thick sections were incubated in 0.3% H_2O_2 (30 min) and autoclaved for 10 min at 121°C in distilled water. After washing three times in PBS, the sections were incubated at room temperature for 1 h with a mouse monoclonal anti-αvβ3 integrin antibody (Millipore) diluted 1:100 in a solution of PBS and 5% skimmed milk. The Dako Cytomation Envision+ System-HRP Kit was then applied according to the manufacturer's protocol (DakoCytomation, Carpentaria, CA, USA). After three washes in PBS, the sections were counterstained with hematoxylin.

For immunofluorescent staining, snap-frozen tissue samples were embedded in a compound of optimal cutting temperature for cryosectioning, and 16-μm cryostat sections were processed for indirect immunofluorescence. The slides were incubated with 10% horse serum in PBS at room temperature for 60 min, then overnight at 4°C with an anti-RECA-1 antibody (Abcam, Cambridge, MA, USA) diluted 1:20 in 1% horse serum in PBS. After three washes with PBS for 5 min, the slides were incubated with a Cy3-conjugated anti-mouse antibody (Jackson ImmunoResearch Laboratories) and DAPI (1:500) (Invitrogen) in PBS for 60 min. The slides were then washed in PBS and mounted.

Statistical analysis

The student's *t* test was used to test for statistical significance. Data were presented as the means ± standard error. Kaplan–Meier curves were compared using the log-rank test.

Statistical analysis was performed using Stat View statistical software (version 5.0; SAS Institute Inc., Cary, NC, USA).

Results

Immunohistochemical analysis of αvβ3 integrin expression in the two glioma cell lines

Immunofluorescence assays were conducted to determine the expression of αvβ3 integrin in J3T-1 and J3T-2 cells. Cultured J3T-1 cells were not immunopositive for αvβ3 integrin (Fig. 1A). In contrast, robust expression of αvβ3 integrin was observed on the surface of J3T-2 cells (Fig. 1B).

Immunohistochemical staining for αvβ3 integrin was also performed in brain slices of animals harboring either J3T-1 or J3T-2 brain tumors. The J3T-1 glioma cells that were clustered around the dilated tumor vessels were negative for αvβ3 integrin, yet the endothelial cells of dilated tumor vessels were clearly positive for αvβ3 integrin (Fig. 1C). J3T-2 glioma cells were diffusely positive for αvβ3 integrin. There were no dilated vessels in the J3T-2 tumors that were positive for αvβ3 integrin (Fig. 1D).

Effects of cilengitide on endothelial cells in vitro

To investigate the effects of cilengitide on endothelial cells, a tube formation assay using HUVECs co-cultured with NHDFs was performed. HUVECs formed tubes in the medium containing VEGF (Fig. 2A). The addition of cilengitide (0.1 μM, 0.5 μM, 1.0 μM) to the culture medium inhibited tube formation in a concentration-dependent manner (Fig. 2B–D). All HUVECs and NHDFs detached from the dishes when the concentration of cilengitide was 2.0 μM. An anti-VEGF drug (suramin: 50 μM) also inhibited tube formation (Fig. 2E). The average tube length under each condition was computed (0 μM cilengitide: $1.45\times10^4 \pm 4.9\times10^2$ pixels; 0.1 μM cilengitide: $1.24\times10^4 \pm 5.8\times10^2$ pixels; 0.5 μM cilengitide: 1.04×10^4

$\pm 5.8\times10^2$ pixels; 1.0 μM cilengitide: $0.90\times10^4 \pm 4.8\times10^2$ pixels ($P < 0.05$); 50 μM suramin: $0.99\times10^4 \pm 6.8\times10^2$ pixels) (Fig. 2F). Quantitative analysis of tube length confirmed that cilengitide inhibited angiogenesis *in vitro* in a concentration-dependent manner.

Cytotoxic effects of cilengitide on the two invasive glioma cell lines in vitro

The direct effects of cilengitide were investigated on glioma cells *in vitro*. J3T-1 and J3T-2 cells were incubated with cilengitide at concentrations of 0–1.0 μM. Treated cells were examined for morphologic changes after 120 h. Originally, J3T-1 cells in culture were composed of bipolar cells and spherical cells. When the cells were incubated with cilengitide, the number of spherical cells increased in a dose-dependent manner (Fig. 3A). However, there was no significant increase in the number of detached cells. Before administration of cilengitide, J3T-2 cells were mostly composed of bipolar cells. They became spherical and agglutinated when cilengitide was added to the incubation media. Some of these deformed cells detached from the plate (Fig. 3A). The detached J3T-2 cells were not viable, as indicated by unsuccessful attempts of re-plating in media containing no cilengitide. To confirm the apoptosis of deformed glioma cells treated with cilengitide, cells were stained with the In Situ Cell Death Detection Kit using TMR red. J3T-1 cells were negative for apoptosis, while J3T-2 cell clusters were positive (Fig. 3B).

The attached cell count was measured and compared between 24 and 120 h after incubation (Fig. 3C). The counts of J3T-1 cells did not change with any concentrations of cilengitide (0–1.0 μM), whereas the counts of J3T-2 cells decreased in a dose-dependent manner. The count of J3T-1 cells incubated with or without cilengitide (1.0 μM) increased by 19.2-fold and 18.9-fold, respectively. The count of J3T-2 cells incubated with or without cilengitide increased by 13.2-fold and 19.6-fold, respectively. Therefore, cilengitide significantly inhibited the proliferation of J3T-2 cells ($P < 0.05$), but not J3T-1 cells ($P =$

0.992).

Anti-angiogenic effects of cilengitide in the J3T-1 gliomas in rats

Angiogenic activity was histopathologically evaluated using the J3T-1 angiogenesis-dependent invasive glioma models in rats. ~~Macroscopic examinations~~ Low magnification of HE staining of J3T-1 control tumors revealed that J3T-1 cells formed clusters in the adjacent normal brain (Fig. 4A). Immunofluorescence staining (vascular endothelial cells: RECA-1, red; nuclei: DAPI, blue) of J3T-1 control tumors clearly showed this tumor's angiogenesis-dependent invasive phenotype as described in a former study[20]. In short, J3T-1 cells were clustered, with these clusters centered on dilated neovascular vessels, and invaded along the perivascular area (Fig. 4C). When animals were treated with intraperitoneal cilengitide (n=3), brain tumors showed an angiogenesis-dependent pattern (Fig. 4B). There was no significant difference in the invasive pattern between cilengitide-treated and control tumors. However, the extent of spread of invasion clusters was significantly decreased in animals treated with cilengitide compared with the control animals. Furthermore, the diameter of the tumor clusters and its core vessels in the treated animals was smaller than that in the untreated animals (Fig. 4D).

To quantify the effect of cilengitide, the diameter of the tumor clusters around the neovasculature and the diameter of the tumor vessels were measured with ImageJ software (http://rsb.info.nih.gov/ij). The diameter of tumor clusters in control and cilengitide-treated animals was 111 ± 6.4 μm and 86.3 ± 6.8 μm, respectively ($P < 0.005$) (Fig. 4E). The diameter of core vessels in control and treated animals was 16.3 ± 1.0 μm and 12.5× ± 1.0 μm, respectively ($P < 0.005$) (Fig. 4F).

Anti-invasive effects of cilengitide demonstrated in the J3T-2 gliomas in rats

The effect of cilengitide on the diffuse invasive activity of glioma cells was histopathologically evaluated using J3T-2 angiogenesis-independent invasive glioma models in rats. Macroscopic examinations of HE staining of J3T-2 control tumors revealed that J3T-2 tumors strongly invaded the adjacent normal brain (Fig. 5A). Briefly, tumor cells gradually dispersed from the tumor center to the normal brain parenchyma with a cell density gradient, which meant that J3T-2 cells formed poorly demarcated tumors. Minimal angiogenesis was seen with only a small number of slightly dilated vessels at the tumor center. A similar invasive pattern was observed in animals treated with cilengitide (n=3) (Fig. 5B). The merged immunofluorescence staining images (vascular endothelial cells: RECA-1, red; nuclei: DAPI, blue) revealed the tumor borders in more detail (Fig. 5C, D). The distribution area of diffuse tumor cell infiltration around the tumor center was smaller in cilengitide-treated animals compared with control animals. To quantify the cell density, the merged images from the J3T-2 tumor center to the normal subcortex, avoiding the corpus callosum, were partitioned into 22 equal areas (200 μm×100 μm), and the nuclei (DAPI, blue) in each area were counted (n=3). The cell density at the tumor center was significantly higher in treated animals than in control animals (Fig. 5E). The cell density of control tumors was gradually reduced from the tumor center toward the normal brain parenchyma, while the cell density of treated tumors dropped steeply at the tumor border. There were no significant differences in cell numbers in the designated areas (200 μm×2200 μm) (control tumors: 1400 ± 31 cells; treated tumors: 1310 ± 72 cells; P = 0.27) (Fig. 5F).

The cytotoxic effects of cilengitide on the J3T-1 and J3T-2 gliomas in rats

The cytotoxic effects of cilengitide on glioma cells *in vivo* were investigated using both rat brain tumor models. A subpopulation of apoptotic cells were visualized by the TdT-mediated dUTP nick end labeling (TUNEL) treatment using the In Situ Cell Death Detection Kit

(apoptotic cells: TMR red; nuclei: DAPI, blue). The J3T-1 control tumor (Fig. 6A), J3T-1 cilengitide treated tumor (Fig. 6B), J3T-2 control tumor (Fig. 6C), and J3T-2 cilengitide treated tumor (Fig. 6D) sections from rat brains were prepared and assayed. These figures show a low number (2-3%) of apoptotic cells. To quantify the cytotoxic effect of cilengitide, the number of apoptotic cells per high-power field (HPF) in J3T-1 tumors (Fig.6E) and J3T-2 tumors (Fig.6F) were assessed. (J3T-1 control tumors: 5.75 ± 1.6 cells/HPF, J3T-1 cilengitide treated tumors: 3.71 ± 0.6 cells/HPF, J3T-2 control tumors: 4.50 ± 1.1 cells/HPF, J3T-2 cilengitide treated tumors: 5.83 ± 1.1 cells/HPF). There was no significant difference in apoptotic cells in the cilengitide-treated tumors compared with control tumors (J3T-1, $P = 0.5972$; J3T-2, $P = 0.4233$).

Survival analysis by using two different invasive glioma models

To evaluate the *in vivo* anti-tumor effect of cilengitide, the long-term survival of mice harboring J3T-1 or J3T-2 brain tumors was analyzed. Athymic mice harboring J3T-1 or J3T-2 brain tumors (12 animals each) were each divided into two groups. The animals received either intraperitoneal cilengitide (200 μg/100 μL, three times/week) or PBS. The median survival was 57.5 days in animals bearing J3T-1 tumors treated with cilengitide, and 31.8 days in animals given PBS (Fig. 7A). A significant prolongation of survival by cilengitide administration was observed in animals harboring J3T-1 tumors ($P < 0.005$). In contrast, the survival of mice bearing J3T-2 gliomas was not prolonged by intraperitoneal cilengitide injection ($P = 0.69$) (Fig. 7B). The median survival of the animals with J3T-2 tumors treated either with cilengitide or PBS was 48.9 days or 48.5 days, respectively.

Discussion

In the present study, we tested cilengitide on two invasive glioma animal models, J3T-1

(αvβ3 integrin-negative, angiogenesis-dependent invasive phenotype) and J3T-2 (αvβ3 integrin-positive, angiogenesis-independent invasive phenotype). *In vitro* proliferation of αvβ3 integrin-positive J3T-2 cells was significantly inhibited by cilengitide, whereas cilengitide treatment did not inhibit proliferation in αvβ3 integrin-negative J3T-1 cells. On the other hand, the survival of mice harboring J3T-1 tumors treated with cilengitide was significantly longer than control animals. Although the survival of mice harboring J3T-2 tumors treated with cilengitide was not prolonged, pathologic examination revealed that angiogenesis-independent, single-cell infiltration was clearly inhibited by cilengitide. These results mean that cilengitide has multi-modal anti-glioma mechanisms. This is the first study to show the bimodal mechanisms of the anti-tumor effect of cilengitide on glioma by using two animal invasive brain tumor models.

Cilengitide inhibited the adhesion and proliferation of αvβ3 integrin-positive J3T-2 cells in culture. Apoptosis of J3T-2 cells was also induced due to the loss of adherence to the plate, which is termed anoikis[24]. Cilengitide induces anoikis in brain tumor cells by inhibiting the phosphorylation of FAK, Src, and Akt[17,18]. However, the results from our *in vivo* experiments did not show the cytotoxic effect of cilengitide on J3T-2 cells. As shown by pathological examination of animal brain tumors treated with cilengitide, apoptotic cell numbers did not increase in the integrin-positive J3T-2 brain tumor model. Furthermore, the survival of animals harboring J3T-2 gliomas was not prolonged by cilengitide. To our knowledge, there is no published data which shows cilengitide-induced anoikis in animal brain tumor models. This discrepancy between *in vitro* and *in vivo* results might be partly due to the difference in the dependency of adhesion molecules and the microenvironment. Many adhesion molecules other than αvβ3 integrin, such as cadherins and L1, might be involved in cell-cell or cell- extracellular matrix (ECM) adhesion *in situ* compared with the *in vitro* environment[25,26]. Therefore, blockade of only αvβ3 integrin cannot induce complete

detachment of cells from surrounding tissues and subsequent anoikis.

Angiogenesis is the formation of new blood vessels by the rerouting or remodeling of existing ones, and is the primary method of vessel formation in gliomas. In this study, the efficient inhibition of angiogenesis was shown by the tube formation assay of HUVECs *in vitro*. Furthermore, prolonged survival after cilengitide administration was shown in animals harboring J3T-1 brain tumors, an angiogenesis-dependent invasive glioma model, but not in J3T-2 tumors, an angiogenesis-independent invasive glioma model. Yamada et al. reported that cilengitide is highly effective in suppressing blood vessel growth, thereby inhibiting the orthotopic growth of human GBM cells in animals[27]. Angiogenesis requires three distinct steps: 1) blood vessel breakdown; 2) degradation of the vessel basement membrane and the surrounding ECM; and 3) migration of endothelial cells and the formation of new blood vessels[3]. During the third step, endothelial cells proliferate and begin to migrate toward tumor cells expressing pro-angiogenic compounds. Endothelial cell activation up-regulates the expression of cell surface adhesion/migration molecules, especially αvβ3 integrin, which results in an enhancement of endothelial cell adhesion and migration[12,13]. Cilengitide might prevent the third step of angiogenesis and reduce the size of tumor vessels. Thus, the anti-angiogenic effects of cilengitide are likely the main mechanism inhibiting angiogenic J3T-1 tumor growth.

Previously it was reported that there is a shift from the angiogenic to the invasive phenotype after anti-angiogenic therapy with use of an anti-VEGF antibody[28-31]. Invasion is another target for glioma therapy and glioma cell invasion requires four distinct steps: 1) detachment of invading cells from the primary tumor mass; 2) adhesion to the ECM; 3) degradation of the ECM; and 4) cell motility and contractility[3]. During the second step, integrins allow glioma cells to adhere to the ECM. αvβ3 integrin, which binds to fibronectin, vitronectin, and tenascin-C in the ECM, plays a central role in glioma invasion[15]. Platten et al.

reported that inhibition of αvβ3 integrin decreased glioma cell motility *in vitro*[32]. Cilengitide might inhibit this second step, thereby suppressing the invasiveness of the glioma. This is the first study to show that cilengitide suppresses the angiogenesis-independent, single-cell infiltration of glioma cells in the animal J3T-2 brain tumor model. However, cilengitide had no survival benefit on J3T-2 brain tumors. This was because cilengitide had little direct cytotoxic effect on tumor cells in situ.

In the invading front of the glioma, most of the arteries have an intact blood-brain barrier (BBB) because single cell invasion is angiogenesis-independent[20]. Therefore, drugs must pass through the normal BBB to exert anti-invasive effects on invading cells. According to our results treating J3T-2 brain tumors with cilengitide, the drug apparently passes through the normal BBB. In a North American Brain Tumor Consortium (NABTC) study, increased intra-tumoral cilengitide levels were shown in patients with glioblastoma when cilengitide was administered 24 h before surgical debulking. This study confirms that cilengitide is effectively delivered into primary human GBM tumors[33].

To analyze the mechanisms of angiogenesis and invasion of gliomas, and anti-glioma effects of drugs which target them, animal models which show angiogenic tumor growth or diffuse invasive growth are required. However, most of the conventional animal models show angiogenic tumor growth but fail to mimic the diffuse invasiveness of human glioma[3]. Therefore, analysis of the invasive ability of glioma has depended on *in vitro* evaluation systems. We have established two novel invasive animal glioma models, J3T-1 and J3T-2, from the same parental cells that separately reflect these two invasive phenotypes of human malignant gliomas[20,4]. J3T-1 gliomas demonstrate angiogenesis-dependent invasive growth that is limited to the perivascular space of newly developed blood vessels. On the other hand, J3T-2 gliomas showed angiogenesis-independent, diffusely invasive growth. The expression levels of integrins are also different between these models; J3T-1 is αvβ3

integrin-negative, while J3T-2 is αvβ3 integrin-positive.

These models were used to investigate the anti-angiogenic and anti-invasion effects of cilengitide separately. The most notable characteristics of our models, which make them ideal for studying cilengitide, are as follows. First, J3T-1 and J3T-2 brain tumor models histologically recapitulate both the invasive and angiogenic phenotypes observed in human glioma. Human gliomas consist of mixtures of these phenotypic subclones[20]. To clarify the anti-glioma mechanisms, models that exhibit each phenotype separately are needed. Second, J3T-1 and J3T-2 brain tumor models are easily reproducible. Third, they consist of subclones established from the same parental cell. Thus, they should have similar genetic backgrounds (T Maruo et al., Proteomics-based analysis of invasion-related proteins in malignant gliomas, submitted).

In this study, the anti-invasive effect of cilengitide was shown in animal brain tumor models. Also, the lack of a direct cytotoxic effect of cilengitide was demonstrated in animal models. Yamada et al. tested cilengitide in a U87 brain tumor model in mice[27]. Since U87 cells show well-demarcated, angiogenic, and non-invasive growth *in vivo*, Yamada and colleagues could only examine the anti-angiogenic effect of cilengitide, but could not test an anti-invasive effect or a cytotoxic effect. Therefore, an *in vivo* evaluation system such as our paired invasive glioma models is necessary for the evaluation of novel therapeutic agents.

The formation of abnormal tumor vasculature and single-cell invasion into normal brain parenchyma are major reasons for the resistance of malignant glioma to conventional treatments. Our results showed that cilengitide exerts a bimodal anti-glioma effect with anti-angiogenic and anti-invasive effects. Therefore, cilengitide holds promise as a glioma therapy in the clinical setting.

There have been several reports that showed preliminary results of phase I or II study of cilengitide for recurrent or newly diagnosed malignant glioma. Cilengitide monotherapy or

combination treatment with radiation and/or temozolomide is well tolerated and exhibits modest anti-tumor activity[34].

Bevacizumab, another anti-angiogenic agent, is a humanized monoclonal antibody against vascular endothelial growth factor that demonstrates a strong anti-angiogenic effect in gliomas. However, bevacizumab induces a phenotypic shift in the glioma from angiogenic to diffusely invasive tumors leading to therapy-resistant tumor progression[28-31]. According to results from a limited number of studies, such phenotypic shift is not reported after cilengitide treatment. This might be partly because of cilengitide's bimodal anti-angiogenic and anti-invasive effects.

According to our results, cilengitide has a strong anti-tumor effect which is mainly dependent on the anti-angiogenic and anti-invasive effects but has little, if any, direct cytotoxic effect on glioma cells. Therefore, combination therapy with cytotoxic therapeutics, e.g., radiation therapy, other chemotherapy, or oncolytic virus therapy, would be effective. Alghisi et al. demonstrated that cilengitide elicits signaling events that disrupt vascular endothelial (VE)-cadherin localization at cellular contacts and increases the permeability of the endothelial monolayer. Therefore, the effects of cilengitide on endothelial cells make it a potentially well-suited drug to be combined with chemotherapeutic agents to improve drug delivery[18]. Several preclinical studies have shown an enhanced anti-tumor effect of cilengitide when administered in combinatorial therapeutic regimens[9,35-37]. The anti-angiogenic effect of cilengitide also may enhance combined treatments. Mikkelsen et al. showed cilengitide did not influence the effect of radiation on U251 glioma cells but strongly amplified effects on endothelial cell survival in vitro. They also showed cilengitide treatment dramatically amplified the efficacy of radiation therapy in an animal glioma model[38]. Kurozumi and colleagues demonstrated the enhanced therapeutic efficacy of an oncolytic virus on experimental glioma with cilengitide pretreatment[39]. They showed oncolytic virus

therapy-induced changes in tumor microenvironment, such as increased tumor vascular permeability, leukocyte infiltration, and inflammatory cytokines, were inhibited by pretreatment with a single dose cilengitide.

Conclusions

In conclusion, our results indicate that cilengitide exerts a phenotypic anti-tumor effect by inhibiting tumor angiogenesis and tumor cell invasion. These two mechanisms are clearly shown by the experimental treatment of two different animal invasive glioma models.

Acknowledgments

This study was supported by grants-in-aid for Scientific Research from the Japanese Ministry of Education, Culture, Sports, Science, and Technology to T.I. (No. 19591675; No. 22591611), and K.K. (No. 20890133; No. 21791364). Cilengitide was generously provided by Merck Serono and the National Cancer Institute, NIH**.** We thank H. Wakimoto, M. Arao, and A. Ishikawa for their technical assistance. The following medical students also contributed to the animal experiments: T. Mifune, S. Murai, M. Matsueda, H. Matsumoto, and Y. Yoshida. Merck Serono has reviewed this publication; the views and opinions described in this publication do not necessarily reflect those of Merck Serono.

References

1. Stupp R, Mason WP, van den Bent MJ, et al. Radiotherapy plus concomitant and adjuvant temozolomide for glioblastoma. *N Engl J Med.* Mar 10 2005;352(10):987-996.

2. Chatterjee S, Matsumura A, Schradermeier J, Gillespie GY. Human malignant glioma therapy using anti-alpha(v)beta3 integrin agents. *J Neurooncol.* 2000;46(2):135-144.

3. Tate MC, Aghi MK. Biology of angiogenesis and invasion in glioma. *Neurotherapeutics.* Jul 2009;6(3):447-457.

4. Onishi M, Ichikawa T, Kurozumi K, Date I. Angiogenesis and invasion in glioma. *Brain Tumor Pathol.* Feb 2011;28(1):13-24.

5. Kerbel R, Folkman J. Clinical translation of angiogenesis inhibitors. *Nat Rev Cancer.* Oct 2002;2(10):727-739.

6. Vredenburgh JJ, Desjardins A, Herndon JE, 2nd, et al. Phase II trial of bevacizumab and irinotecan in recurrent malignant glioma. *Clin Cancer Res.* Feb 15 2007;13(4):1253-1259.

7. Vredenburgh JJ, Desjardins A, Herndon JE, 2nd, et al. Bevacizumab plus irinotecan in recurrent glioblastoma multiforme. *J Clin Oncol.* Oct 20 2007;25(30):4722-4729.

8. de Groot JF, Fuller G, Kumar AJ, et al. Tumor invasion after treatment of glioblastoma with bevacizumab: radiographic and pathologic correlation in humans and mice. *Neuro Oncol.* Mar 2010;12(3):233-242.

9. Reardon DA, Nabors LB, Stupp R, Mikkelsen T. Cilengitide: an integrin-targeting arginine-glycine-aspartic acid peptide with promising activity for glioblastoma multiforme. *Expert Opin Investig Drugs.* Aug 2008;17(8):1225-1235.

10. Varner JA, Cheresh DA. Integrins and cancer. *Curr Opin Cell Biol.* Oct 1996;8(5):724-730.

11. Friedlander M, Brooks PC, Shaffer RW, Kincaid CM, Varner JA, Cheresh DA. Definition of two angiogenic pathways by distinct alpha v integrins. *Science.* Dec 1 1995;270(5241):1500-1502.

12. Brooks PC, Clark RA, Cheresh DA. Requirement of vascular integrin alpha v beta 3 for angiogenesis. *Science.* Apr 22 1994;264(5158):569-571.

13. Brooks PC, Montgomery AM, Rosenfeld M, et al. Integrin alpha v beta 3 antagonists

promote tumor regression by inducing apoptosis of angiogenic blood vessels. *Cell.* Dec 30 1994;79(7):1157-1164.

14. Hodivala-Dilke KM, Reynolds AR, Reynolds LE. Integrins in angiogenesis: multitalented molecules in a balancing act. *Cell Tissue Res.* Oct 2003;314(1):131-144.

15. Leavesley DI, Ferguson GD, Wayner EA, Cheresh DA. Requirement of the integrin beta 3 subunit for carcinoma cell spreading or migration on vitronectin and fibrinogen. *J Cell Biol.* Jun 1992;117(5):1101-1107.

16. MacDonald TJ, Taga T, Shimada H, et al. Preferential susceptibility of brain tumors to the antiangiogenic effects of an alpha(v) integrin antagonist. *Neurosurgery.* Jan 2001;48(1):151-157.

17. Oliveira-Ferrer L, Hauschild J, Fiedler W, et al. Cilengitide induces cellular detachment and apoptosis in endothelial and glioma cells mediated by inhibition of FAK/src/AKT pathway. *J Exp Clin Cancer Res.* 2008;27:86.

18. Alghisi GC, Ponsonnet L, Ruegg C. The integrin antagonist cilengitide activates alphaVbeta3, disrupts VE-cadherin localization at cell junctions and enhances permeability in endothelial cells. *PLoS One.* 2009;4(2):e4449.

19. Tucker GC. Alpha v integrin inhibitors and cancer therapy. *Curr Opin Investig Drugs.* Jun 2003;4(6):722-731.

20. Inoue S, Ichikawa T, Kurozumi K, et al. Novel animal glioma models that separately exhibit two different invasive and angiogenic phenotypes of human glioblastomas. *World Neurosurgery.* in press.

21. Hampl JA, Camp SM, Mydlarz WK, et al. Potentiated gene delivery to tumors using herpes simplex virus/Epstein-Barr virus/RV tribrid amplicon vectors. *Hum Gene Ther.* May 1 2003;14(7):611-626.

22. Bishop ET, Bell GT, Bloor S, Broom IJ, Hendry NF, Wheatley DN. An in vitro model

of angiogenesis: basic features. *Angiogenesis.* 1999;3(4):335-344.

23. Igarashi T, Miyake K, Kato K, et al. Lentivirus-mediated expression of angiostatin efficiently inhibits neovascularization in a murine proliferative retinopathy model. *Gene Ther.* Feb 2003;10(3):219-226.

24. Bouchard V, Demers MJ, Thibodeau S, et al. Fak/Src signaling in human intestinal epithelial cell survival and anoikis: differentiation state-specific uncoupling with the PI3-K/Akt-1 and MEK/Erk pathways. *J Cell Physiol.* Sep 2007;212(3):717-728.

25. Cifarelli CP, Titus B, Yeoh HK. Cadherin-dependent adhesion of human U373MG glioblastoma cells promotes neurite outgrowth and increases migratory capacity. Laboratory investigation. *J Neurosurg.* Mar 2011;114(3):663-669.

26. Izumoto S, Ohnishi T, Arita N, Hiraga S, Taki T, Hayakawa T. Gene expression of neural cell adhesion molecule L1 in malignant gliomas and biological significance of L1 in glioma invasion. *Cancer Res.* Mar 15 1996;56(6):1440-1444.

27. Yamada S, Bu XY, Khankaldyyan V, Gonzales-Gomez I, McComb JG, Laug WE. Effect of the angiogenesis inhibitor Cilengitide (EMD 121974) on glioblastoma growth in nude mice. *Neurosurgery.* Dec 2006;59(6):1304-1312; discussion 1312.

28. Norden AD, Young GS, Setayesh K, et al. Bevacizumab for recurrent malignant gliomas: efficacy, toxicity, and patterns of recurrence. *Neurology.* Mar 4 2008;70(10):779-787.

29. Kunkel P, Ulbricht U, Bohlen P, et al. Inhibition of glioma angiogenesis and growth in vivo by systemic treatment with a monoclonal antibody against vascular endothelial growth factor receptor-2. *Cancer Res.* Sep 15 2001;61(18):6624-6628.

30. Rubenstein JL, Kim J, Ozawa T, et al. Anti-VEGF antibody treatment of glioblastoma prolongs survival but results in increased vascular cooption. *Neoplasia.* Jul-Aug 2000;2(4):306-314.

31. Tuettenberg J, Friedel C, Vajkoczy P. Angiogenesis in malignant glioma--a target for antitumor therapy? *Crit Rev Oncol Hematol.* Sep 2006;59(3):181-193.

32. Platten M, Wick W, Wild-Bode C, Aulwurm S, Dichgans J, Weller M. Transforming growth factors beta(1) (TGF-beta(1)) and TGF-beta(2) promote glioma cell migration via Up-regulation of alpha(V)beta(3) integrin expression. *Biochem Biophys Res Commun.* Feb 16 2000;268(2):607-611.

33. Gilbert MR, Kuhn J, Lamborn KR, et al. Cilengitide in patients with recurrent glioblastoma: the results of NABTC 03-02, a phase II trial with measures of treatment delivery. *J Neurooncol.* Jul 8 2011.

34. Reardon DA, Fink KL, Mikkelsen T, et al. Randomized phase II study of cilengitide, an integrin-targeting arginine-glycine-aspartic acid peptide, in recurrent glioblastoma multiforme. *J Clin Oncol.* Dec 1 2008;26(34):5610-5617.

35. Burke PA, DeNardo SJ, Miers LA, Lamborn KR, Matzku S, DeNardo GL. Cilengitide targeting of alpha(v)beta(3) integrin receptor synergizes with radioimmunotherapy to increase efficacy and apoptosis in breast cancer xenografts. *Cancer Res.* Aug 1 2002;62(15):4263-4272.

36. Abdollahi A, Griggs DW, Zieher H, et al. Inhibition of alpha(v)beta3 integrin survival signaling enhances antiangiogenic and antitumor effects of radiotherapy. *Clin Cancer Res.* Sep 1 2005;11(17):6270-6279.

37. Tentori L, Dorio AS, Muzi A, et al. The integrin antagonist cilengitide increases the antitumor activity of temozolomide against malignant melanoma. *Oncol Rep.* Apr 2008;19(4):1039-1043.

38. Mikkelsen T, Brodie C, Finniss S, et al. Radiation sensitization of glioblastoma by cilengitide has unanticipated schedule-dependency. *Int J Cancer.* Jun 1 2009;124(11):2719-2727.

39. Kurozumi K, Hardcastle J, Thakur R, et al. Effect of tumor microenvironment modulation on the efficacy of oncolytic virus therapy. *J Natl Cancer Inst.* Dec 5 2007;99(23):1768-1781.

Figure legends

Fig. 1. *In vitro* and *in vivo* immunohistochemical analysis of αvβ3 integrin expression in J3T-1 and J3T-2 cells. Immunofluorescence of αvβ3 integrin in cultured cells was negative in J3T-1 cells (A) and positive on the surface of J3T-2 cells (B). Scale bar = 50 μm. Immunohistochemical staining for αvβ3 integrin in brain slices revealed that the J3T-1 glioma cells were negative for αvβ3 integrin, yet the endothelial cells of dilated tumor vessels were positive (C). J3T-2 glioma cells were diffusely positive for αvβ3 integrin (D). Scale bar = 50 μm.

Fig. 2. Effects of cilengitide on tube formation. HUVECs co-cultured with fibroblasts and VEGF (10 ng/mL) without cilengitide (A) or with cilengitide (0.1, 0.5, 1.0 μM) (B-D) or suramin (50 μM) (E) for ten days. The length of tube-like structures was measured quantitatively using an image analyzer. The tube length was significantly shortened with cilengitide treatment in a concentration-dependent manner (*P = 0.0062, **P = 0.0089). (mean ± SE, n = 6)

Fig. 3. Direct cytotoxic effects of cilengitide on the J3T-1 and J3T-2 glioma cells in culture. Morphological changes were observed after cilengitide treatment (0.1, 0.5, or 1.0 μM) in a dose-dependent manner. Some of the J3T-1 cells became spherical but did not detach from the plate (upper panel in A). J3T-2 cells become spherical and agglutinated. Some of the deformed cells detached from the plate (lower panel in A). Deformed cells were stained red

by TUNEL treatment in J3T-2 cells (lower panel in B), but not in J3T-1 cells (upper panel in B). A significant inhibitory effect on the proliferation of J3T-2 cells was observed (*P < 0.005), but was not seen in J3T-1 cells (P = 0.992) (C). (mean ± SE, n = 6)

Fig. 4. Anti-angiogenic effects of cilengitide on the J3T-1 gliomas in rats. ~~Macroscopic examinations~~ Low magnification of HE staining of control tumors (A) and cilengitide-treated tumors (B) revealed the same invasive pattern of cluster formation around dilated neovasculature. However, the spread of the invasion clusters was significantly smaller in animals treated with cilengitide compared with control animals. Scale bar = 2.0mm. When examined with immunofluorescence staining (vascular: RECA-1, red; nuclei: DAPI, blue), the diameter of the tumor clusters and its core vessels in cilengitide-treated animals (D) was smaller than that in untreated animals (C). Scale bar = 100 μm. The quantitative analysis of the diameter of the tumor clusters (E) and its core vessels (F) revealed a significant decrease in cilengitide-treated animals compared with control animals (P＜0.005). (mean ± SE, n = 3)

Fig. 5. Anti-invasive effects of cilengitide on the J3T-2 gliomas in rats. HE staining of control tumors (A) and cilengitide-treated tumors (B) revealed that tumor cells gradually dispersed from the tumor center to the normal brain parenchyma with a cell density gradient in both tumors. Scale bar = 2 mm. Immunofluorescence staining (vascular endothelial cells: RECA-1, red; nuclei: DAPI, blue) of control tumors (C) and cilengitide-treated tumors (D) revealed that the tumor borders of the treated tumors were more evident. Scale bar = 500 μm. The cell density was higher at the center of the tumor and lower at the periphery of the infiltration area in animals treated with cilengitide compared with control animals (E). There were no significant differences in the cell numbers in the examined areas (F) (P = 0.27). (mean ± SE, n = 3)

Fig. 6. Cytotoxic effects of cilengitide on the J3T-1 and J3T-2 rat brain tumors. A subpopulation of apoptotic cells were visualized by TUNEL staining (apoptotic cells: TMR red; nuclei: DAPI, blue) of J3T-1 control tumors (A), J3T-1 cilengitide-treated tumors (B), J3T-2 control tumors (C), and J3T-2 cilengitide-treated tumors (D). Scale bar = 100 μm. The quantitative analysis of the number of the apoptotic cells/HPF in J3T-1 tumors (E) and J3T-2 tumors (F) revealed no significant difference between control and cilengitide-treated animals (J3T-1, P=0.5972; J3T-2, P=0.4233). (mean ± SE, n = 6)

Fig. 7. Survival of athymic mice harboring J3T-1 or J3T-2 brain tumors treated with cilengitide. Kaplan–Meier survival analysis of athymic mice harboring intracranial J3T-1 (A) and J3T-2 (B) brain tumors treated with cilengitide or PBS. The survival time of J3T-1 glioma mice was significantly prolonged by the intraperitoneal injection of cilengitide (A) ($P < 0.005$) while the survival of J3T-2 glioma mice was not prolonged (B) ($P = 0.6889$).

Fig.1

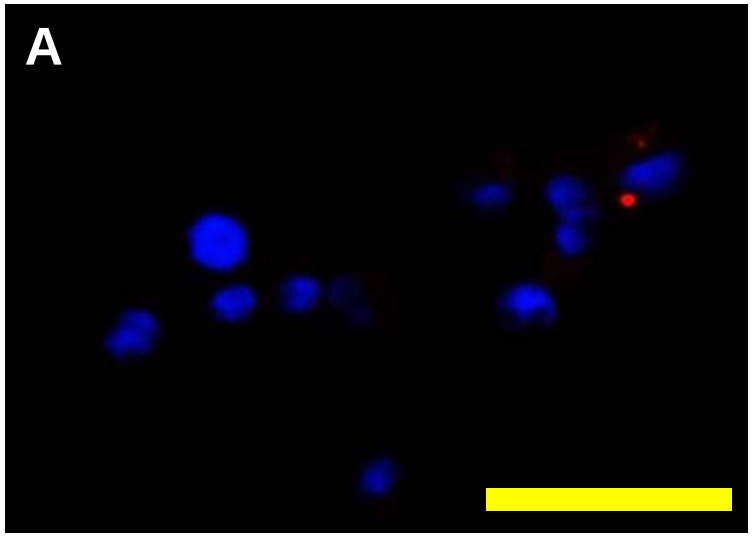

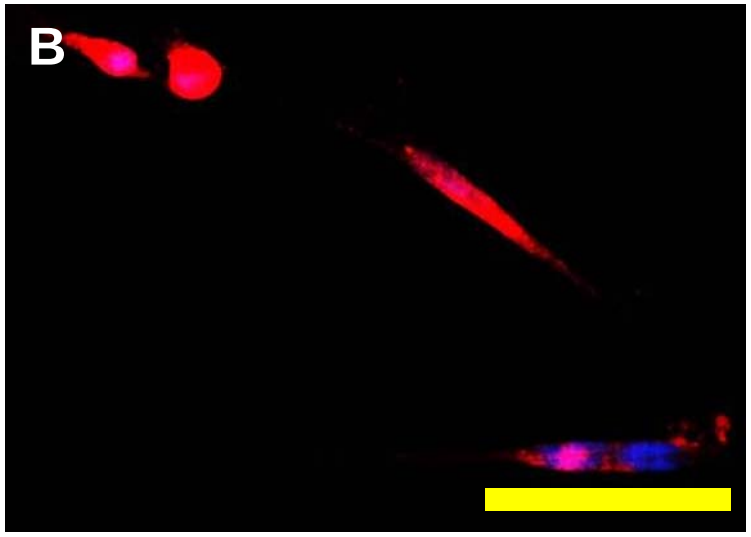

cultured cell
αvβ3 integrin
(red)
DAPI (blue)

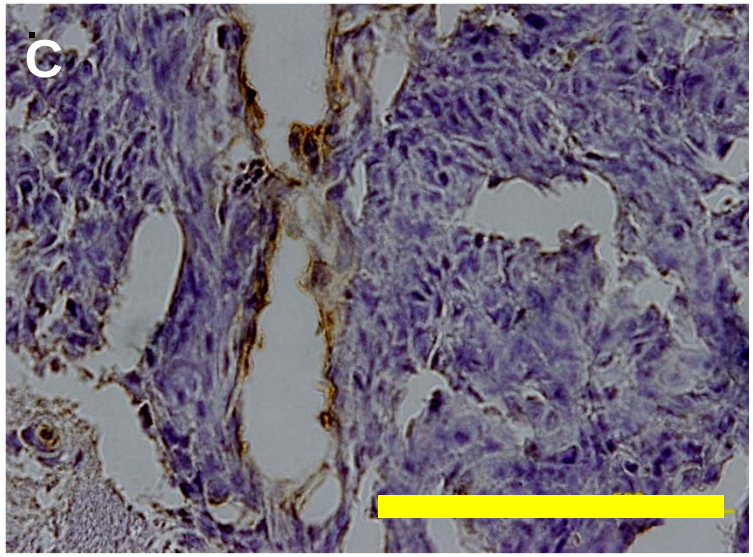

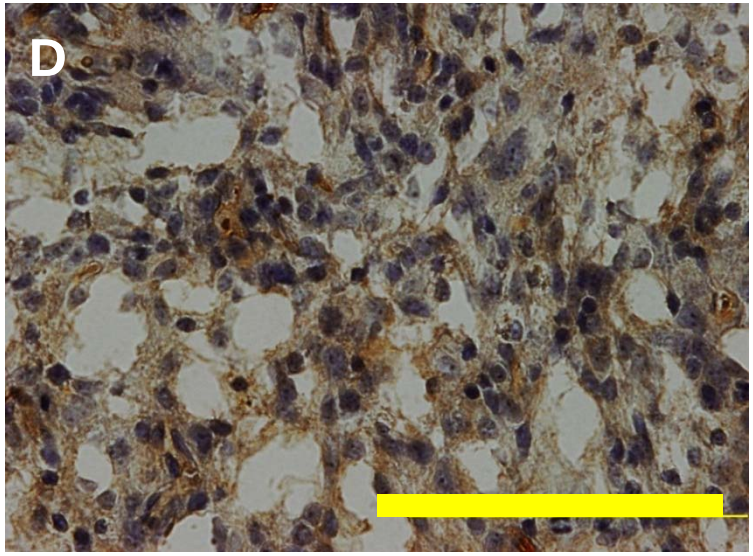

brain tumor
αvβ3 integrin
(DAB)

J3T-1

J3T-2

Fig.2A-E

control

cilengitide 0.1μM

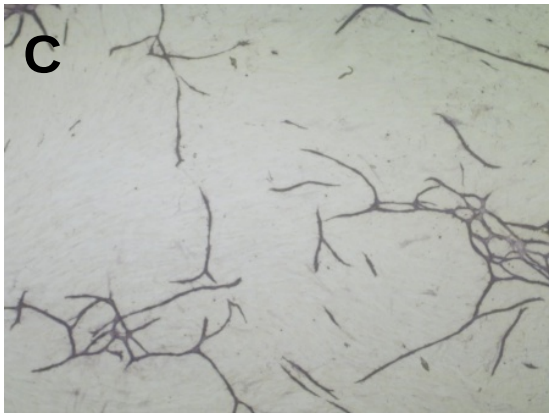

cilengitide 0.5μM

cilengitide 1.0μM

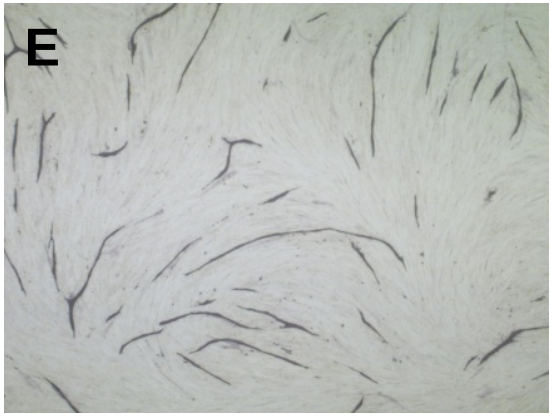

Suramin 50μM

Fig.2F

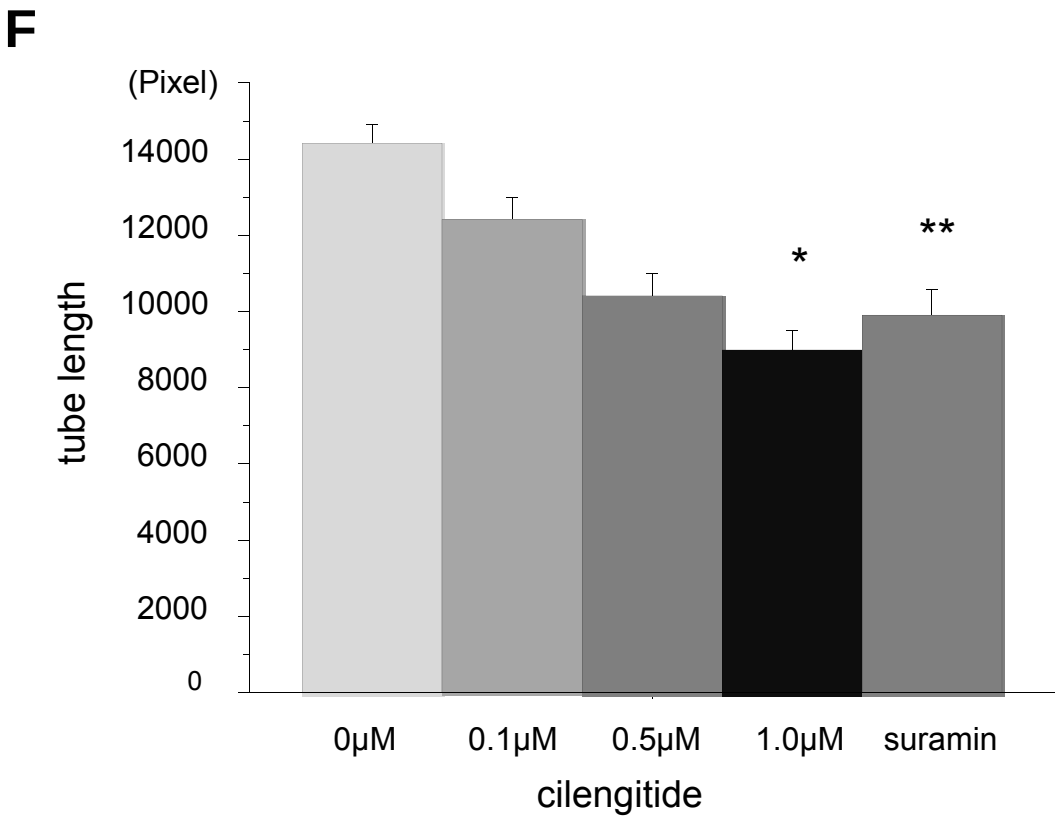
F
(Pixel)
14000
12000
10000
8000
6000
4000
2000
0
tube length
*
**
0μM
0.1μM
0.5μM
1.0μM
suramin
cilengitide

Fig.3A

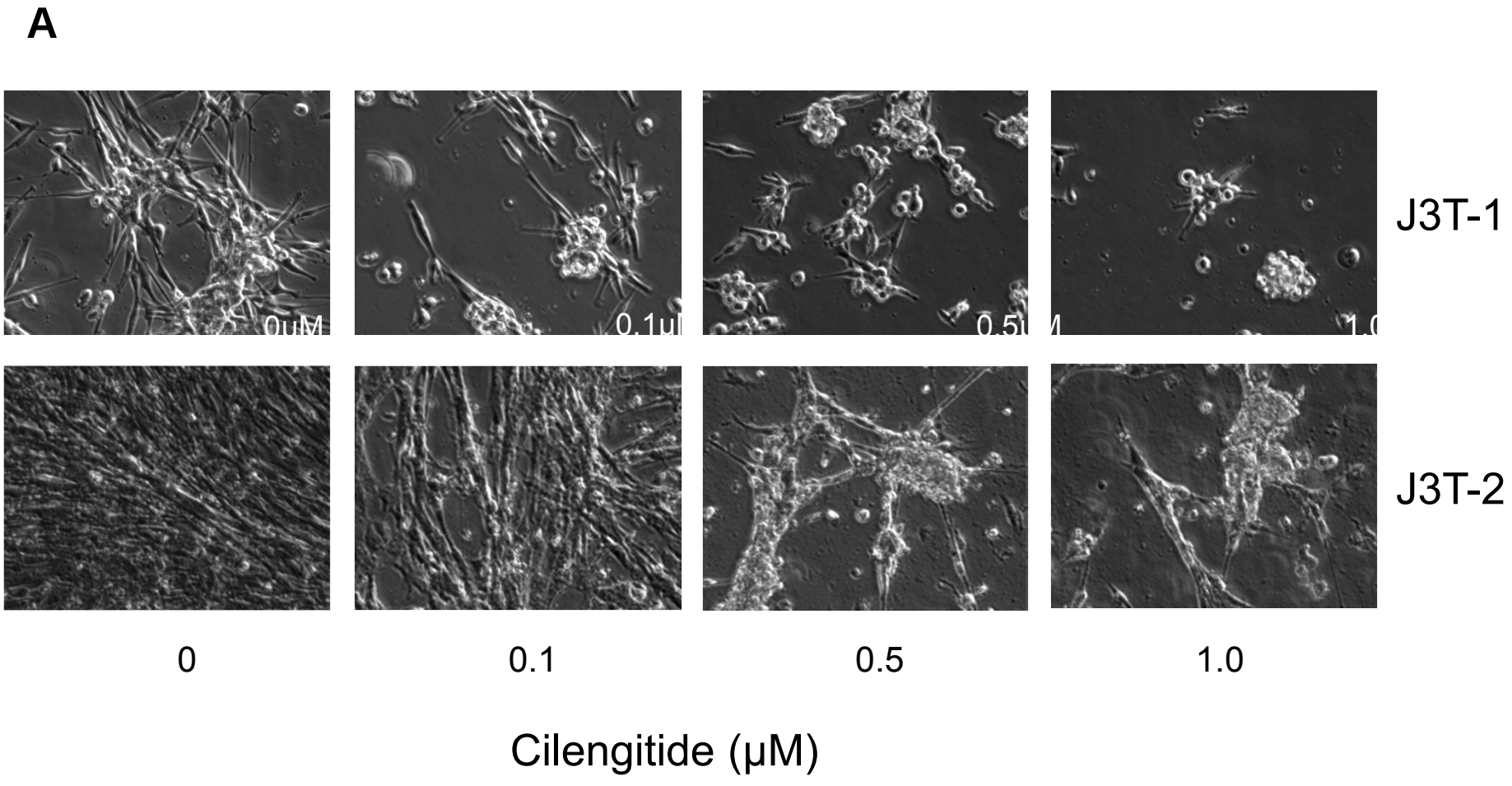

Fig.3B

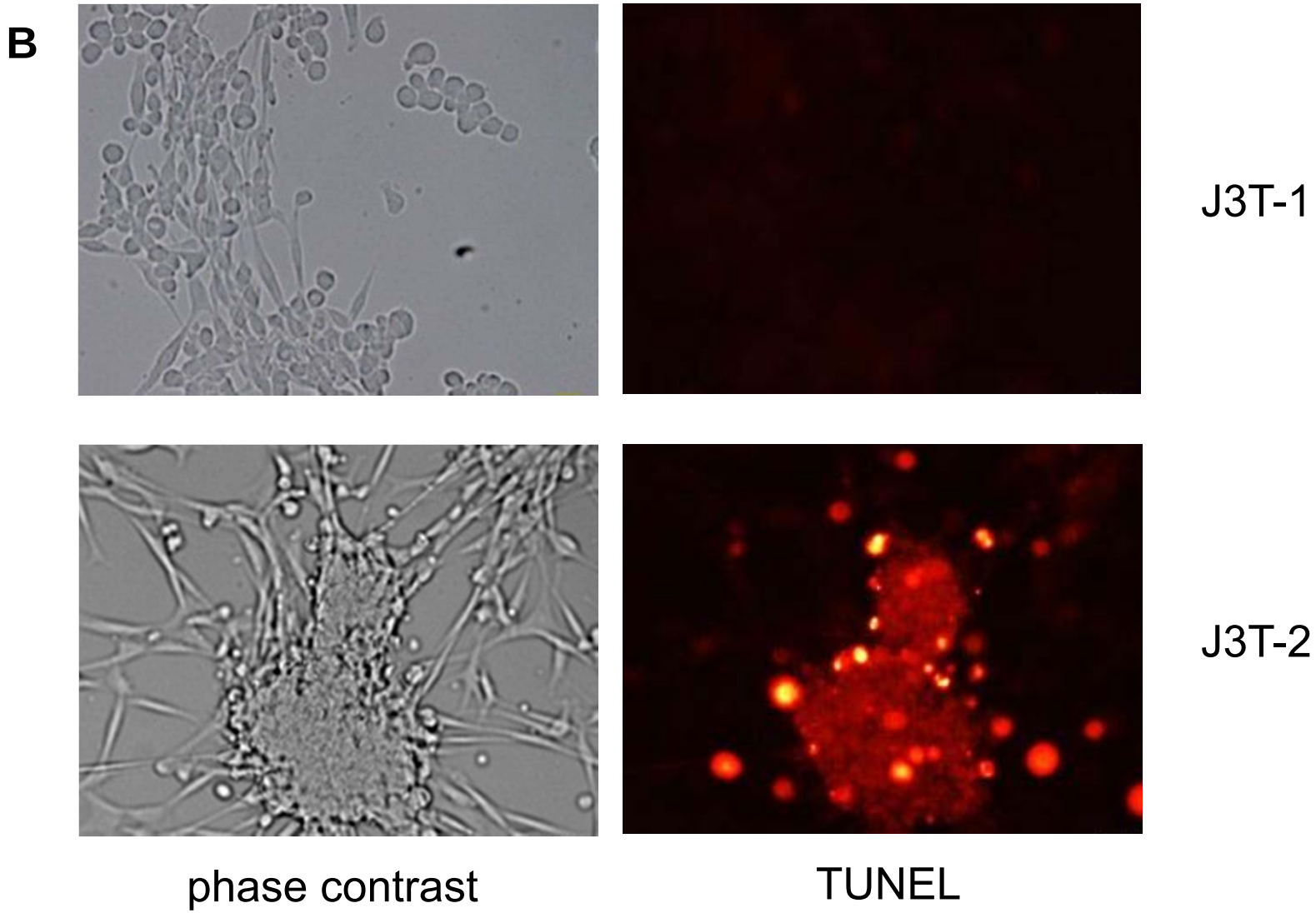

Fig.3C

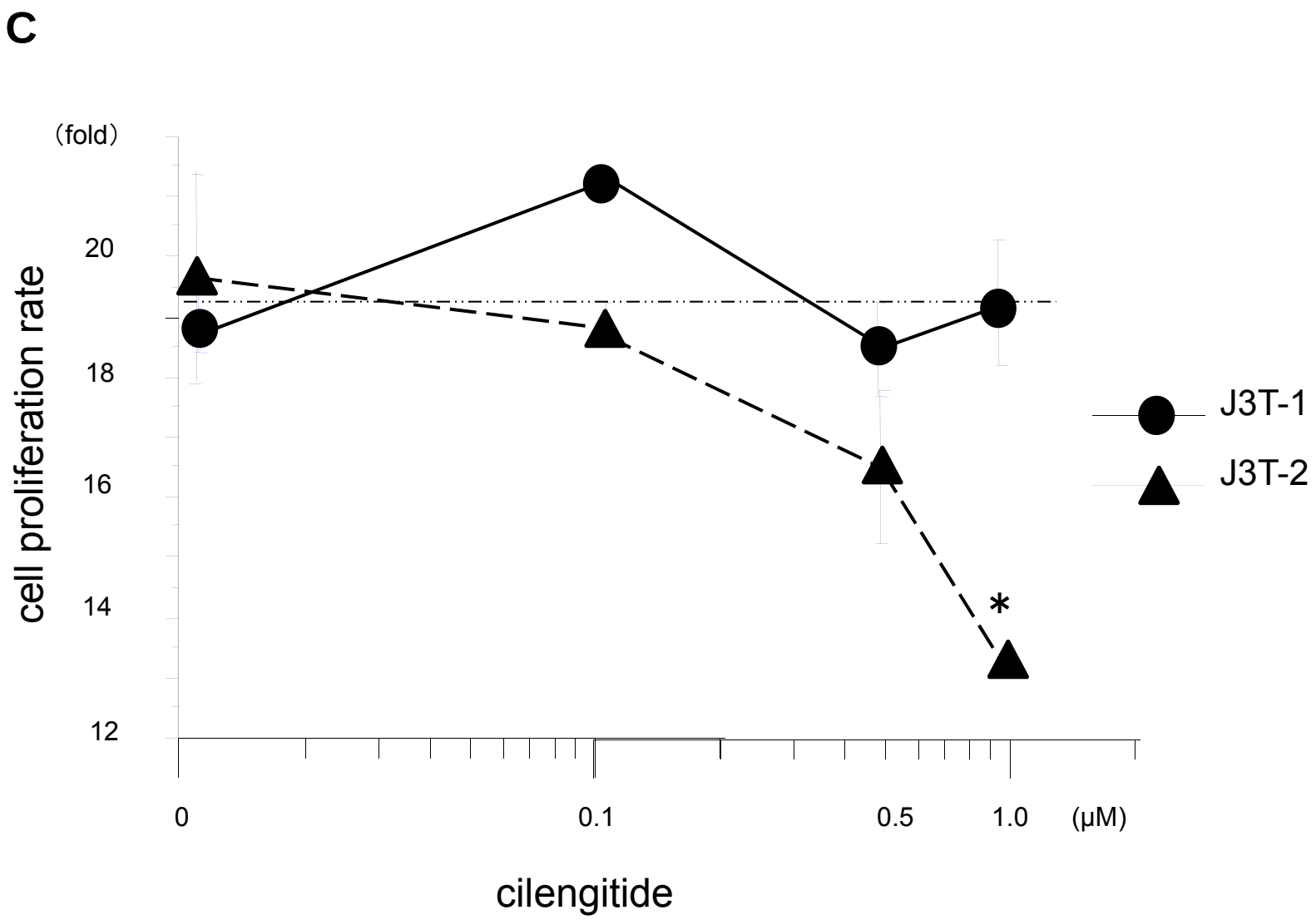
C
(fold)
cell proliferation rate
20
18
16
14
12
0
0.1
0.5
1.0
(μM)
cilengitide
J3T-1
J3T-2
*

Fig.4A-D

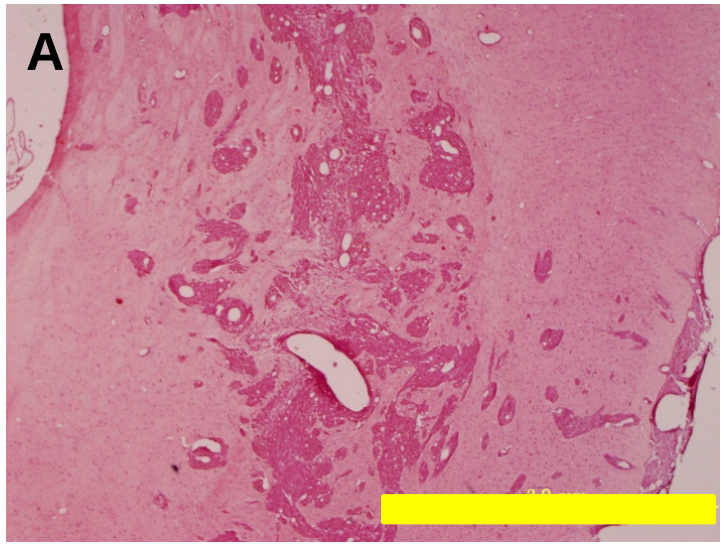

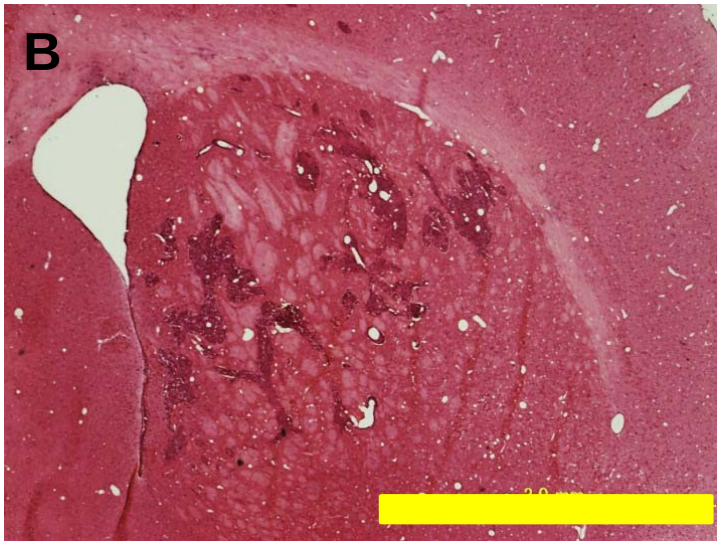

HE

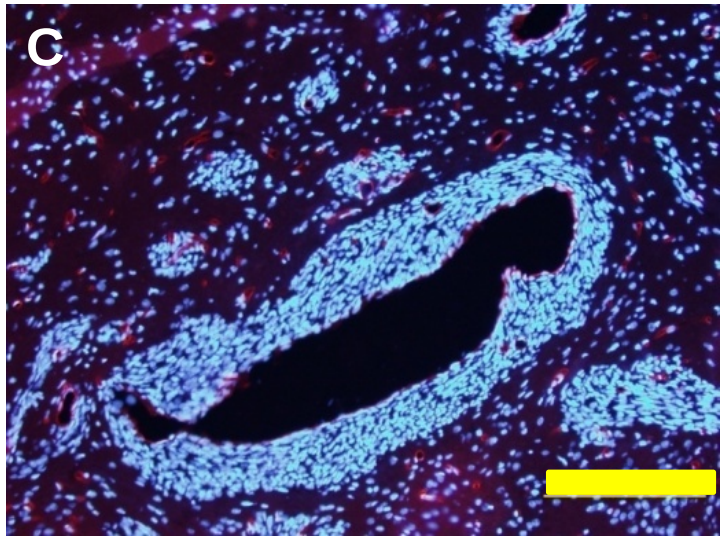

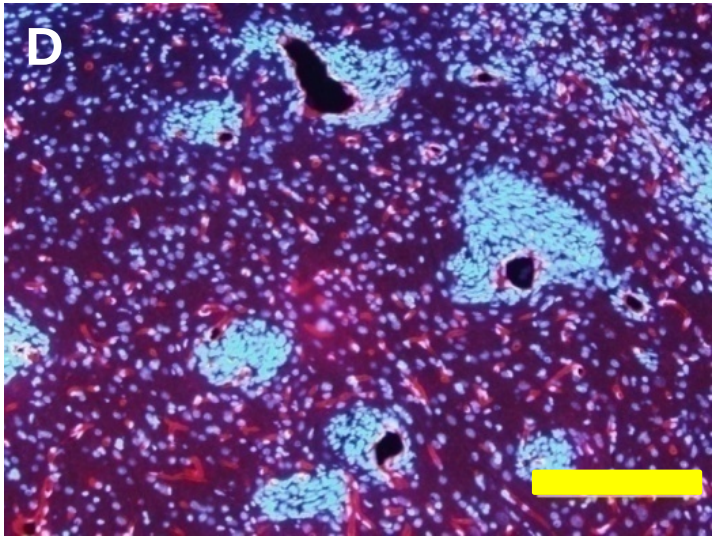

DAPI(blue),
RECA-1(red)

control

cilengitide-treated

Fig.4E, F

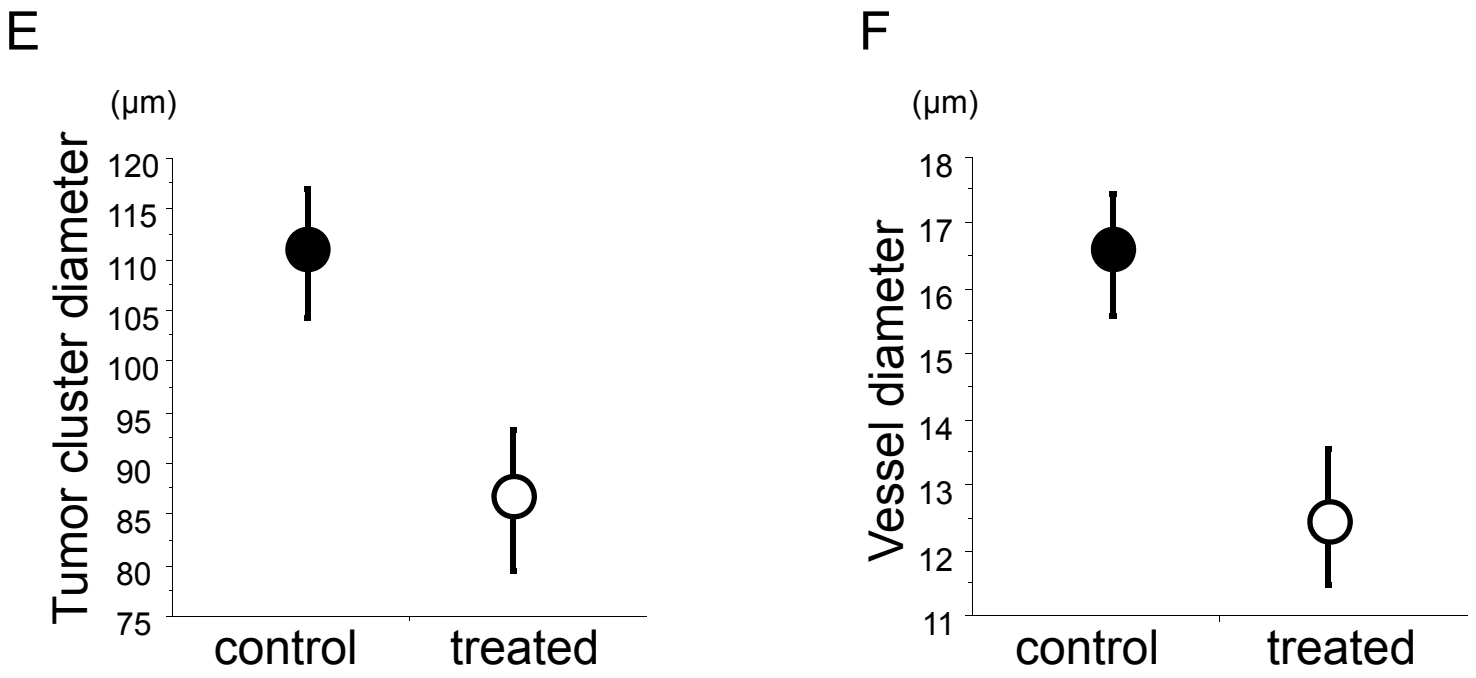
E
(μm)
Tumor cluster diameter
120
115
110
105
100
95
90
85
80
75
control
treated
F
(μm)
Vessel diameter
18
17
16
15
14
13
12
11
control
treated

Fig.5A-D

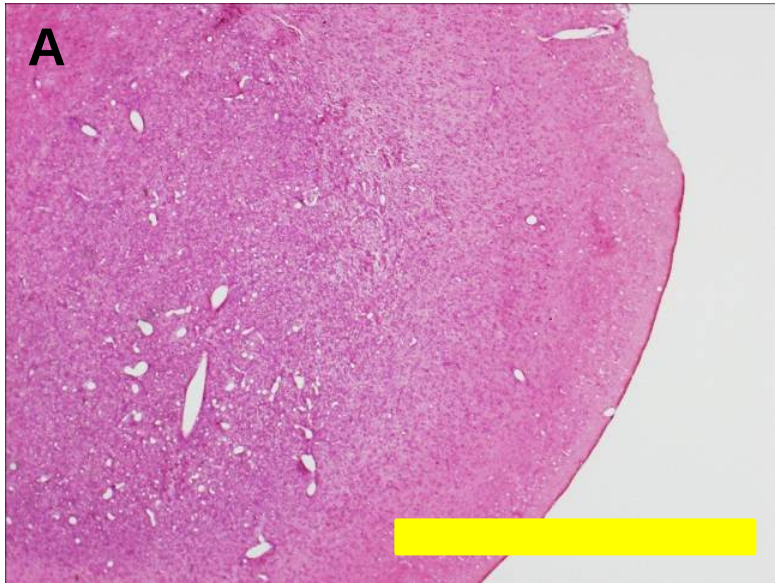

control

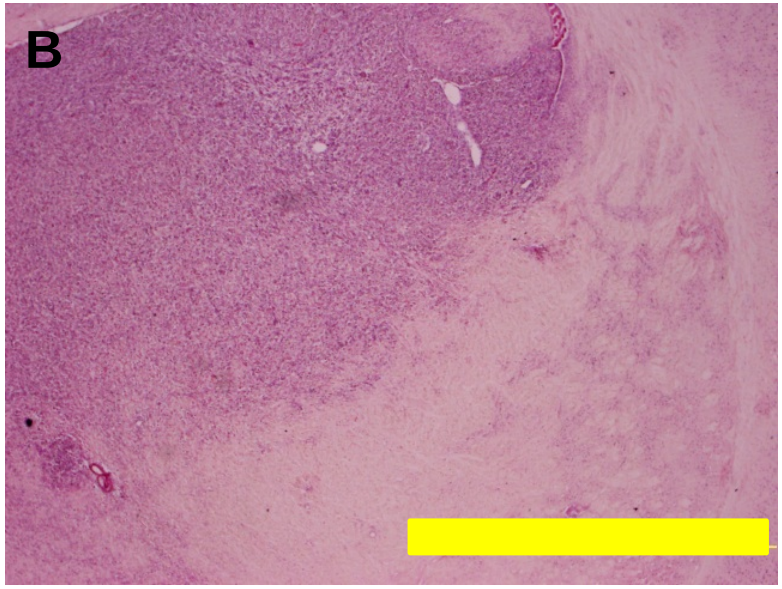

cilengitide-treated

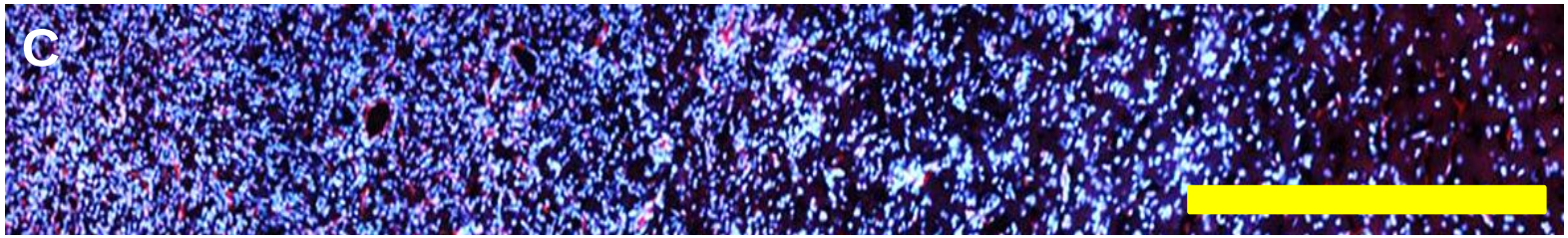

control

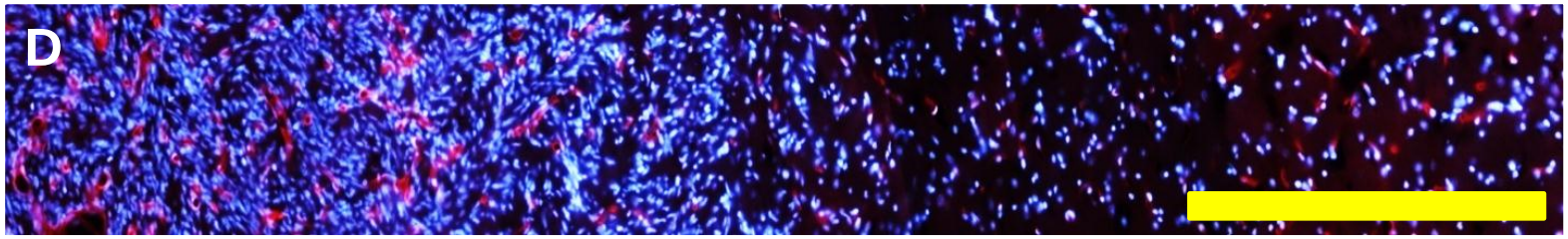

cilengitide-treated

Fig.5E, F

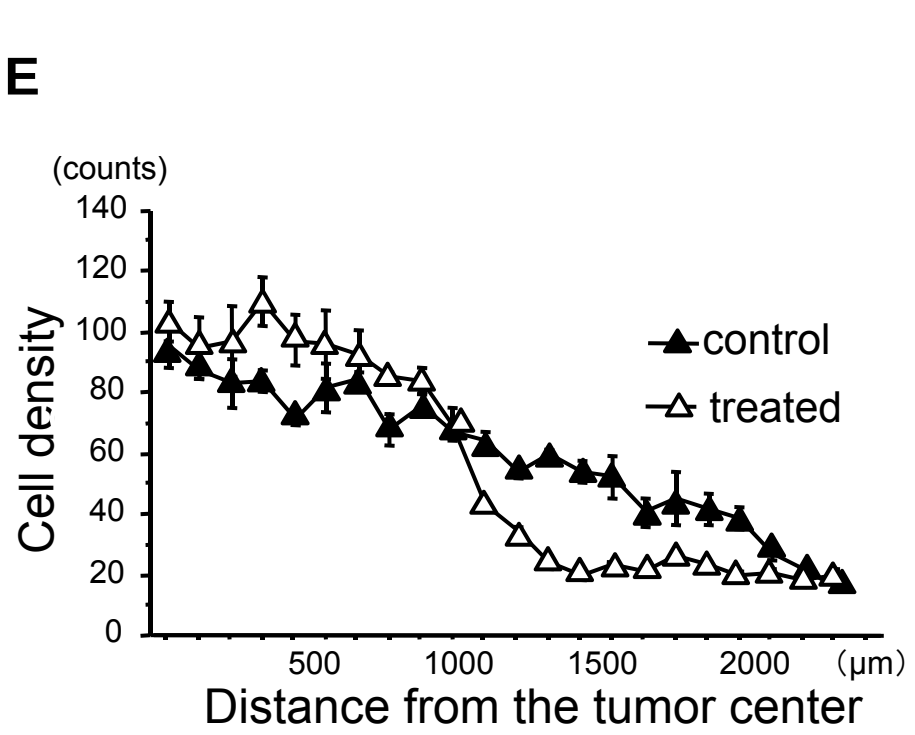
E
(counts)
140
120
100
80
60
40
20
0
Cell density
control
treated
500
1000
1500
2000
(μm)
Distance from the tumor center

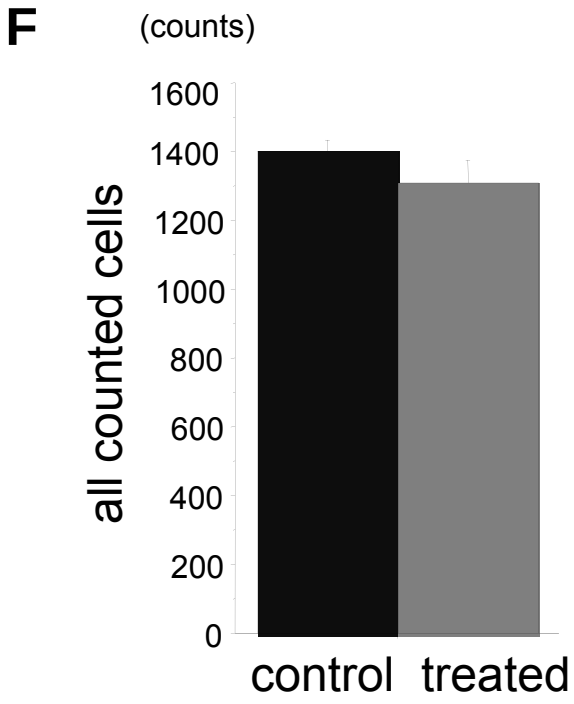
F
(counts)
1600
1400
1200
1000
800
600
400
200
0
all counted cells
control
treated

Fig.6A-D

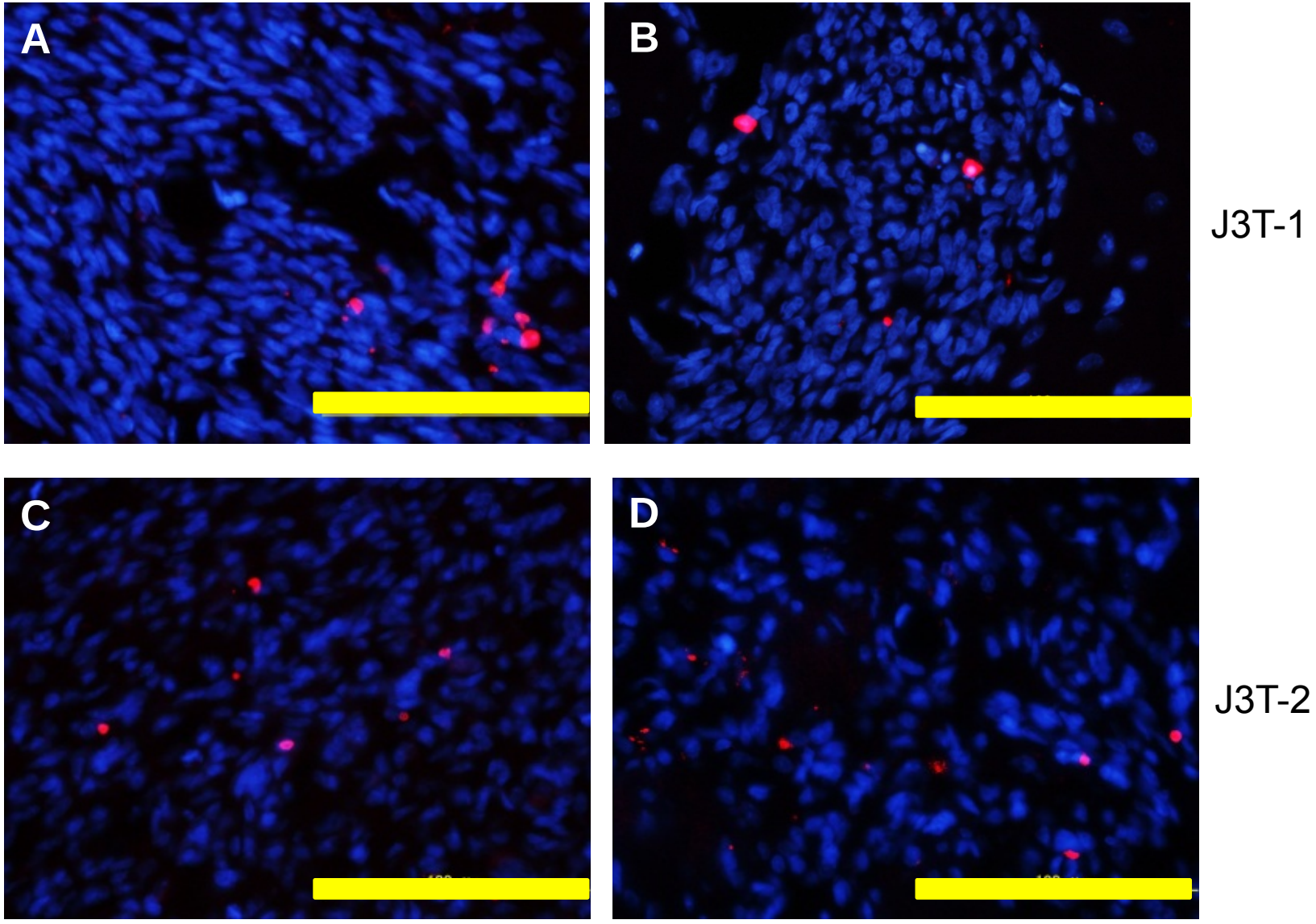

Fig.6E, F

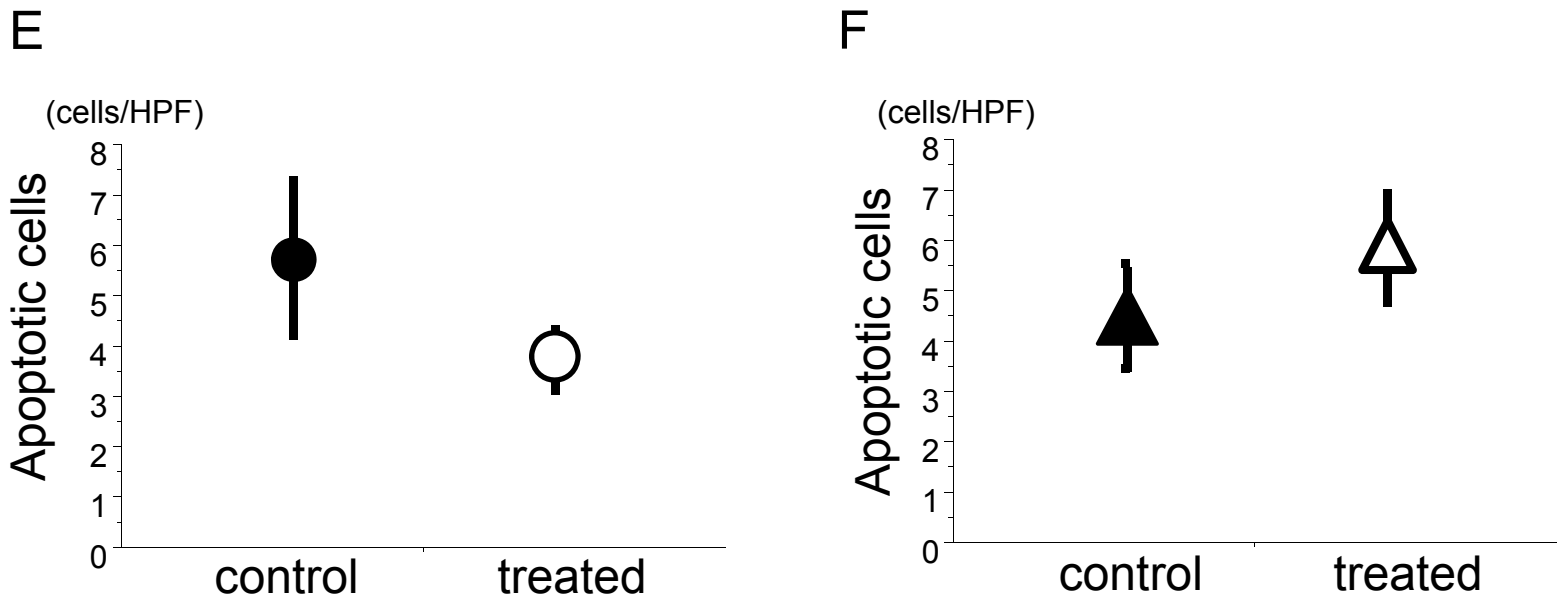
E
(cells/HPF)
Apoptotic cells
8
7
6
5
4
3
2
1
0
control
treated
F
(cells/HPF)
Apoptotic cells
8
7
6
5
4
3
2
1
0
control
treated

Fig.7

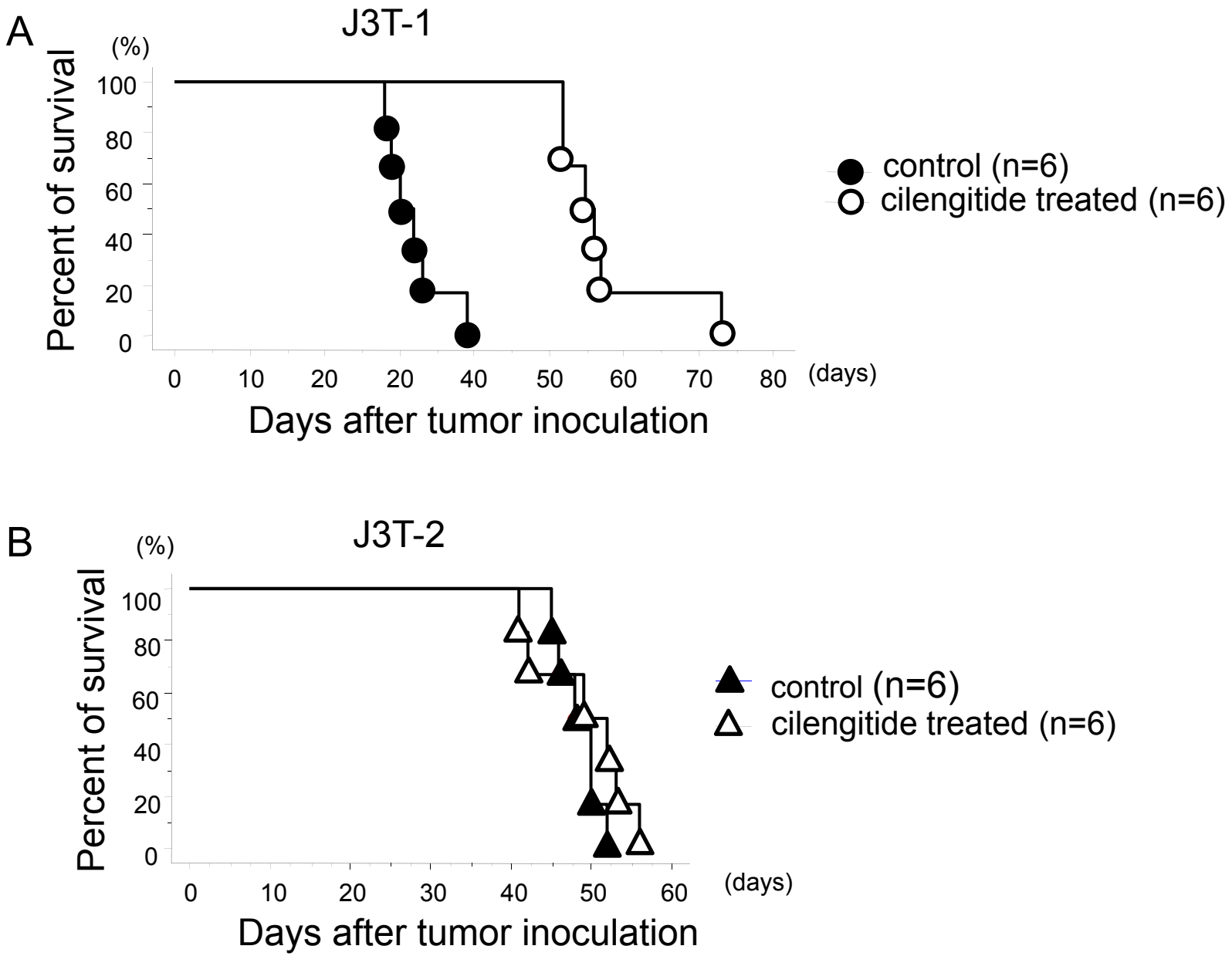
A
J3T-1
(%)
Percent of survival
100
80
60
40
20
0
0
10
20
20
40
50
60
70
80
(days)
Days after tumor inoculation
control (n=6)
cilengitide treated (n=6)
B
J3T-2
(%)
Percent of survival
100
80
60
40
20
0
0
10
20
30
40
50
60
(days)
Days after tumor inoculation
control (n=6)
cilengitide treated (n=6)